ELSEVIER

Journal of Power Sources 53 (1995) 127–135

JOURNAL OF POWER SOURCES

Separator design for valve-regulated lead/acid batteries

B. Culpin

Chloride Industrial Batteries Limited, PO Box 5, Clifton Junction, Swinton, Manchester M27 8LR, UK

Accepted 3 August 1994

Abstract

The wide commercial acceptance of valve-regulated lead/acid batteries for stand-by power applications over the last decade has involved the use of a novel separator material that is based on glass microfibre. The fibre material's exceptionally small diameter (0.5–1 μm), high porosity (95%), zero contact angle, high anisotropy and good compressibility makes it significantly different from conventional flooded separators and, therefore, worthy of detailed study. Nevertheless, very little has been published on the mechanisms by which the electrolyte is retained and the oxygen transported within these nearly saturated recombination systems. This paper reviews critically some of the present methods for characterizing the glass-microfibre materials and suggests improved testing methods that reflect more accurately the subsequent effects on battery performance.

Keywords: Glass-microfibre separator; Valve-regulated lead/acid batteries; Wetting; Stratification; Permeability

1. Introduction

Perhaps the greatest advance in lead/acid technology during the past decade has been the introduction of the valve-regulated lead/acid (VRLA) cell that is designed with immobilized electrolyte and glass-microfibre (GMF) separation [1]. In the 1970s, McClelland and Devitt at the Gates Rubber Company [2] introduced the wound cell that operated on this principle. Since then, the concept of the VRLA has been developed by others into a variety of products that cover the markets for small portable, stand-by and automotive lead/acid batteries [3]. At present, most major battery manufacturers have at least one VRLA product range.

The major technical advance that gave rise to this proliferation of products was the introduction of the GMF-based separator, a material whose many unique properties make it ideally suited to VRLA applications. The material has a high porosity (typically 95%) and, consequently, can absorb a large volume of acid; it has the low pore size necessary for any separator; the structure is 100% glass which gives high chemical resistance and zero contact angle (good wetting characteristics); the fibre is highly compressible so that it can conform to the plate surface with subsequent good acid transfer and low internal resistance [3,4]. These properties have ensured that the required separators have used GMF exclusively. Although efforts have been made to find alternative materials [5], to data, no viable alternatives have reached the market place, except for some types that contain a small proportion of non-glass fibres [6].

Glass microfibre is made from borosilicate glass via a flame-attenuation process that produces a fibre with a diameter in the range from 0.25 to 4 μm, and with a typical length of 1 mm as determined by the diameter [7]. At this stage, the material has the consistency of cotton wool and is processed into sheet form by a wet-laying process on a conventional paper-making machine. This gives the sheet a three-dimensional anisotropy by which most of the fibres lie in the plane of the sheet (x, y orientations) with a slight preference to the machine direction. The anisotropy promotes differences in tensile properties in the three directions and, more importantly, in the pore structure. The effect of pore-size anisotropy has been investigated in a previous paper [8] and is considered to be important in the mechanism of gas transport through the separator at high degrees of saturation. The latter study also demonstrated the usefulness of the Washburn equation in evaluating wicking behaviour. The work reported here continues this investigation by examining the effect of the separator's fibre composition on the wicking characteristics.

In use, the separator has to support a column of acid up to the top of the plate without any variation in saturation. This ability is usually assessed via a wicking

SSDI 0378-7753(94)01982-2

test. Although wicking can provide some information on the pore size of the separator, most batteries are filled from the top so that the separator does not have to wick, but rather it has to resist the drainage of acid. There is little published information on the drainage characteristics of GMF [6] and, therefore, the results of our investigations are reported here.

Pore size is usually assessed by the maximum bubble-pressure technique. When in use in the cell, the separator is under compression. Although this compression is expected to cause a reduction of pore size, no quantitative measure has hitherto been reported. A test method to measure pore size as a function of compression has been developed here and the results for a range of fibre mixes are presented.

Although drainage measures both the ability of the separator to support its electrolyte to a given height and the effect of height on saturation, the ability of the separator to resist concentration stratification is an equally important factor [9]. A good resistance to stratification is of particular importance as the normal gassing charge, that is employed in flooded cells to mix the electrolyte, cannot be used in VRLA designs. A test method to measure the permeability of the separator, which reflects its ability to resist stratification, has been developed and results are reported that demonstrate how this property varies with the fibre mix.

2. Wicking measurements

2.1. Method

The normal wicking test consists of measuring, as a function of time, the progress of the liquid front up a strip of separator that is held vertically with its lower end immersed in the wetting liquid. The test can be performed with the separator in the unrestrained state, or with it compressed between two sheets of transparent plastic. It is normally assumed that wicking occurs at a constant 100% saturation, although unpublished data collected in the author's laboratory have shown this to be incorrect.

For the results presented here, the separator (length 140 mm, width 20 mm) was tested in an uncompressed state in 1.280 sp. gr. acid. Duplicate runs were conducted on a range of GMF separators that contained two, different, fibre diameters.

2.2. Results

The wicking characteristics of a wetting liquid in a porous structure can be described by the Washburn equation. This relates the wicking velocity, v, at a given height to other properties of the system [10], namely:

$$v = \frac{dh}{dt} = \frac{2r\gamma \cos\theta}{8\eta h} - \frac{r^2 \rho q}{8\eta} \quad (1)$$

Integration of Eq. (1) gives:

$$\frac{r^2 \rho q t}{8\eta} = h_m ln\left(\frac{h_m}{h_m - h}\right) - h \quad (2)$$

where h_m is the maximum height reached at infinite time [11], i.e.:

$$h_m = \frac{2\gamma \cos\theta}{\rho g r} \quad (3)$$

Integration of Eq. (1), ignoring the gravity term, yields [12–14]:

$$h^2 = \frac{\gamma r t \cos\theta}{K^2 2\eta} \quad (4)$$

Eq. (4) predicts that for values of $h \ll h_m$, the wicking height h^2 plotted against t should give a linear relationship with a gradient, for perfectly wetting systems ($\theta = 0°$), of $\gamma r / K^2 2\eta$.

The results for the range of fibre mixes studied are shown in Fig. 1 for wicking heights of up to 12 cm ($h^2 = 144$ cm^2). A good linear relationship, as predicted by the Washburn equation, was established. By substituting standard values into Eq. (4), the individual slopes can be converted into equivalent pore sizes (in the direction of wicking). These have been plotted in Fig. 2 as a function of the fibre mix. The property that governs the wicking rate at low values of h is the capillary pressure, P, as defined by the Laplace equation [15,16], namely:

$$P = \frac{2\gamma \cos\theta}{r} \quad (5)$$

Replotting Fig. 2 as fibre mix against $1/r$ gives a straight line, as shown in Fig. 3. This demonstrates clearly that the properties of fibres in a two-component mix are related linearly to capillary pressure.

A demonstration of the wicking characteristic when h is not $\ll h_m$ is given in Fig. 4, in which the behaviour

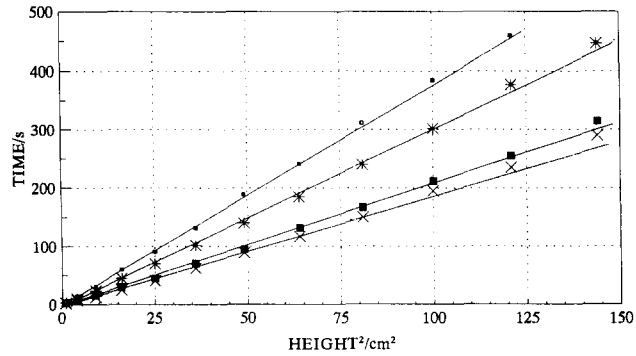

Fig. 1. Effect of fibre mix on wicking characteristics. Percentage of fine fibres: (□) 100, (*) 50, (■) 10, (×) 0.

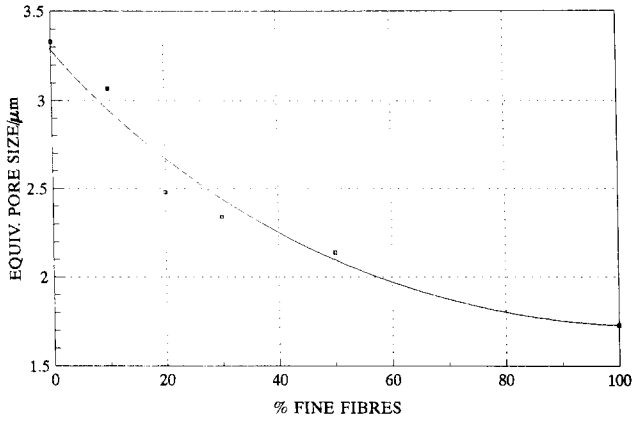

Fig. 2. Effect of fibre mix on pore size.

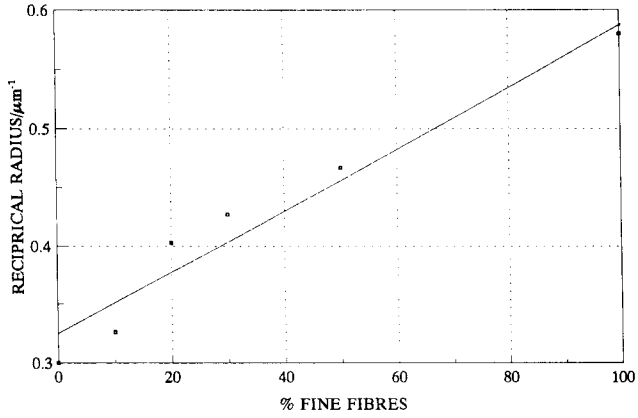

Fig. 3. Effect of fibre mix on capillary pressure.

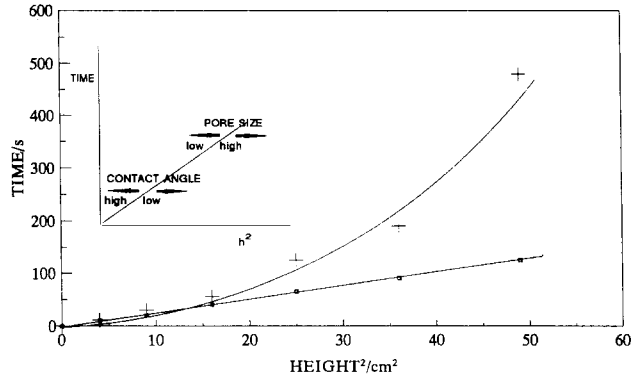

Fig. 4. Comparison of wicking characteristics of glass and non-glass fibre-based separators: (□) GMF, (+) non-glass.

of a GMF separator is compared with that of a non-glass separator material. The linear portion of the curve extends up to a wicking height of only 4 cm for the non-glass material.

2.3. Discussion

The wicking characteristic of a separator can be used to calculate the pore size in the wicking direction (i.e., along the x- and y-coordinates) from the Washburn equation. This assumes, however, that the pore structure consists of circular cross section, parallel-sided capillaries. In fact, scanning electron microscopy (SEM) studies of GMF separators show that this is far from reality [3]. A value of the tortuosity, K, must also be assumed. For a GMF with such a high porosity, the value is conveniently (and, probably, accurately) taken to be unity. Consequently, the values of the pore size thus obtained are best considered to be those of an 'equivalent' pore size, i.e., the pore size of a cylindrical capillary that would have the same wicking properties as the separator. Hence, the actual values obtained (viz., in the order of 2 μm) should be considered with care.

Of particular interest, however, is the linear relationship shown in Fig. 3. This enables the wicking characteristics of any binary mix of fibre diameters to be determined by measuring the wicking rates of only two mixes, ideally: 100% fibre A and 100% fibre B. It is interesting to speculate on the information that might be obtained from a similar treatment of fibre mixes that contain three components, or more.

The non-glass separator was manufactured from fibres with a diameter greater than that of the glass-based separators and, consequently, would be expected to have larger pore sizes. The Washburn equation predicts that a separator with larger pores would wick faster (but with a smaller h_m) as demonstrated in Fig. 1, but this is not found in Fig. 4. The other factor involved in the velocity of wicking is the contact angle. This was $>0°$ for the non-glass material. The effect of the contact angle is to reduce the wicking rate. Since the contact angle of sulfuric acid on the fibre is probably different to that of the bulk material, an accurate value of equivalent pore size is not available from this calculation. The same complication would exist for separators made from a mixture of glass and other fibres with non-zero contact angles.

3. Drainage in the compressed state

3.1. Method

The separator under test (length 600 mm, width 20 mm) was maintained under compression between two sheets of poly(vinyl chloride) (PVC) that were held together at regular intervals by bolts. The correct constant separation between the sheets was assured by placing shims down the length of each side of the test rig (Fig. 5). Horizontal slots were machined at 100 mm intervals down the length of the PVC support pieces. This enabled the separator to be cut into six 100 mm pieces, whilst still in the vertical plane. Such an arrangement prevents any possible redistribution of acid

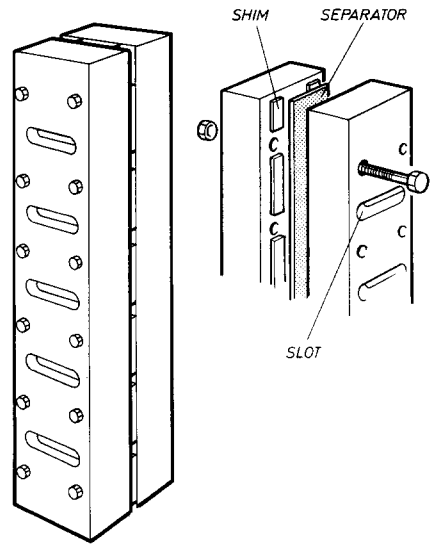

Fig. 5. Test rig for compressed wicking experiments.

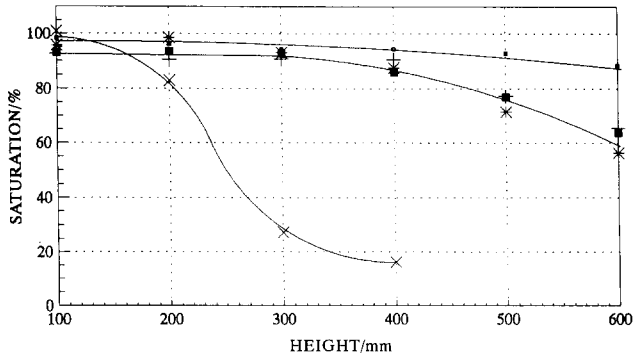

Fig. 6. Effect of time on compressed drainage. Days on test: (□) 8, (+) 14, (*) 21, (■) 28; (×) non-glass.

down the length of the separator during dismantling of the rig at the end of the test.

The procedure was to saturate the separator test piece with 1.280 sp. gr. sulfuric acid, assemble it into the rig, then seal the rig into a polythene bag with 1.280 sp. gr. acid in the bottom (to eliminate any evaporative losses). The rig was suspended in the vertical plane for the required time period. Finally, the separator was cut into 100 mm lengths (whilst still vertical), the assembly dismantled, and the individual pieces weighed.

3.2. Results

The results (expressed as % saturation) were calculated from the glass and acid weights present and are shown graphically in Fig. 6 for one grade of separator material, together with a non-glass material for comparison. The superior electrolyte-retention characteristics of GMF are readily seen. Nevertheless, even GMF has a significant limitation in its ability to resist drainage; it displays a time-dependent reduction in saturation over 400 mm and the time required to reach equilibrium is 14 days. This a better characteristic than that reported by Crouch and Reitz [17] who quote an 80% saturation level at 380 mm after 17 days on test.

3.3. Discussion

Electrolyte drainage from the separator in a fully-assembled cell would be expected to reduce performance, particularly at low discharge rates where acid starvation would limit capacity. Consequently, drainage imposes a maximum height for the element if optimum capacity is to be retained. For the grade of separator tested here, 400 mm is the maximum height that is suggested. The non-glass separator would be expected to exhibit low capacity in any cell. In this respect, the drainage test is superior to the wicking test which, as normally used, is unable to take into account saturation levels. The wicking test could be modified by measuring saturation as a function of height. This was demonstrated by Zguris et al. [6] but results were presented only for heights up to 170 mm and for short periods (4 min).

For cylindrical, parallel-sided capillaries, the maximum wicking height will be the same as the equilibrium drainage height. As already mentioned, this is not a very accurate representation of the pore structure of GMF. To account for the saturation effect, the simple capillary model has to be modified to include a spectrum of capillary diameters that each wick (or drain) to a different height. Furthermore, SEM examination of GMF separators shows that the pore structure does not approach that of a set of parallel-sided capillaries and strongly suggests quite an irregular pore structure [3]. This contributes to problems of capillary-rise hysteresis [18–21] by virtue of the following factors: (i) the difference between a receding and an advancing contact angle, particularly on a rough surface; (ii) the variability in pore geometry, and (iii) the interaction between the contact angle and the pore geometry. All these effects combine to give a drainage height that is greater than a wicking height, as illustrated in Fig. 7. Moreover, as cells are normally filled from the top, drainage represents a more realistic measure of the separator's ability to retain electrolyte.

Although the drainage method can be used for ranking separator performance in terms of an ability to retain a vertical column of electrolyte, direct transfer of these results to cell design should be approached with caution. The drainage characteristics are expected to be modified in assembled cells because the separator is in intimate contact with the porous active material of both positive and negative plates, and these pores are generally smaller than the separator pores.

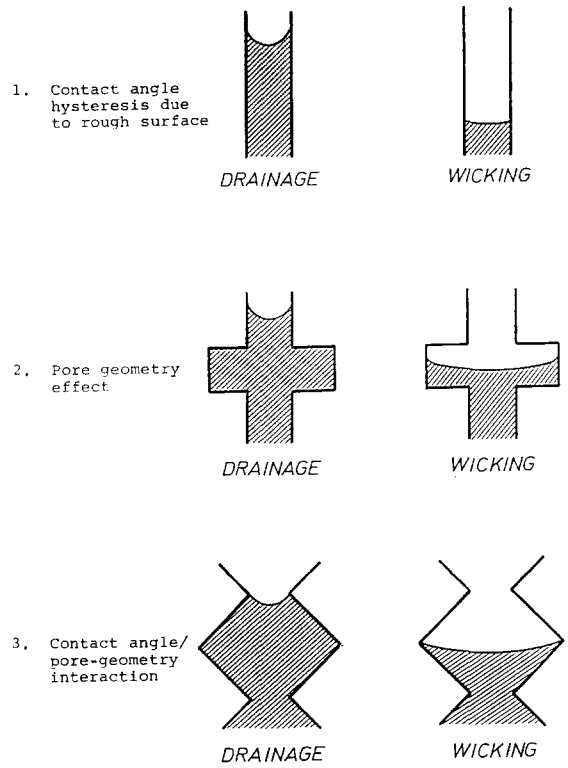

Fig. 7. Factors affecting capillary-rise hysteresis.

4. Drainage in free state

4.1. Method

Strips of separator (length 400 mm, width 20 mm) were saturated with 1.280 sp. gr. sulfuric acid, suspended in a vertical position, and sealed in glass cylinders to prevent evaporative losses. It was found impossible to use longer pieces because of the low tensile strength of the wetted material. At regular time intervals, sample strips were removed and cut into 100 mm pieces whilst retaining their vertical orientation to stop any acid redistribution. The individual pieces were weighed and their thickness measured.

4.2. Results

The data, expressed as saturation against height, show a similar trend to the compressed wicking and give a saturation of about 90% at 400 mm (Fig. 8). The system equilibrated rapidly. The results after three days were similar to those after 1.5 years and this illustrates the long-term stability of the separator system. The actual weight distribution of acid, however, was more pronounced than that observed with compressed wicking, as shown in Fig. 9. The retention of similar saturation levels was obtained by reducing the separator thickness near the top; in fact the separator strip formed a wedge shape with a thickness that decreased gradually from 3.10 mm at the bottom to 2.80 mm at the top.

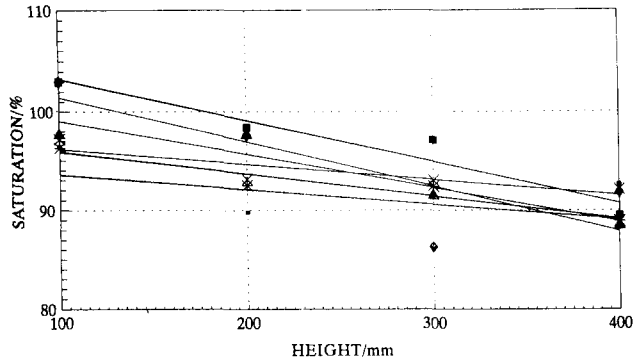

Fig. 8. Effect of time on free drainage. Days on test: (□) 3, (*) 47, (■) 63, (×) 75, (♦) 217, (▲) 548.

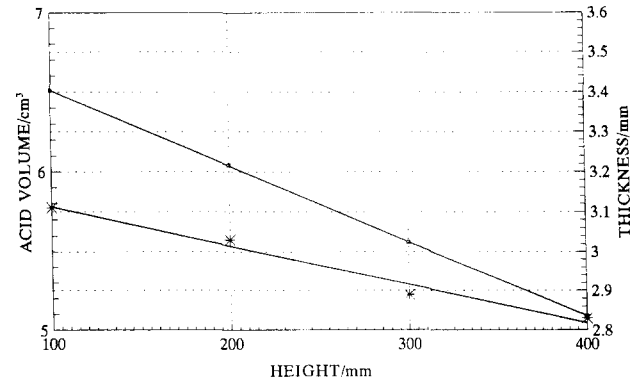

Fig. 9. Thickness effect; 14-day result for free drainage: (□) acid volume, (*) thickness.

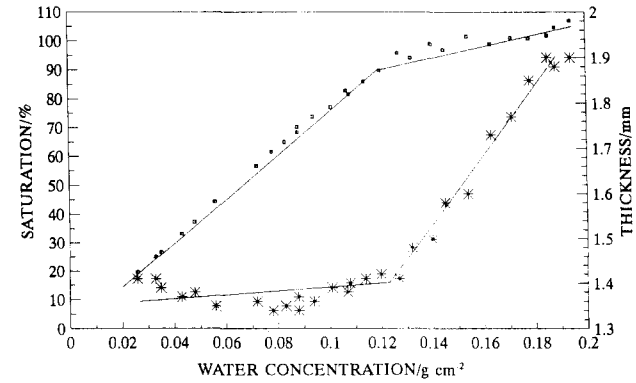

Fig. 10. Saturation vs. thickness: (□) saturation, (*) thickness.

This phenomenon was investigated further by saturating a piece of separator with water and measuring the thickness over a period of hours as the water was allowed to evaporate. The results (presented in Fig. 10) for one grade of separator were unexpected, namely, the drying out takes place in two stages. First, the thickness reduces rapidly to just below the nominal value (measured at 10 kPa) at a constant saturation of 100%; second, the thickness remains constant and the saturation declines, eventually, to zero.

4.3. Discussion

The phenomenon, highlighted by Fig. 10, can be explained by the interplay of two forces, namely, capillary pressure and compressive strength. When the separator is saturated, the liquid/air glass three-phase boundary is at a minimum. As drying out proceeds, the system has two options. If thickness is maintained, the porosity will increase; the large pores will empty first, followed by the smaller ones. This will increase the area of the three-phase boundary and, thereby, will increase the capillary pressure. Such a situation is energetically unfavourable compared with the alternative, which is to reduce the thickness. At a critical state, the force required for compression (the compressive strength) exceeds the capillary pressure and the second stage proceeds at a relatively constant thickness with continually reducing saturation.

Evidence for this mechanism is obtained by considering a similar experiment for a non-glass separator where the capillary pressure is much less owing to both the greater pore size and the greater contact angle; this is shown in Fig. 11. In this case, the drying-out process is accompanied by only a very small reduction in thickness (the capillary pressure is much less but the compressive force is similar to GMF) and there is a continued reduction in saturation. In practical terms, such behaviour has implications for the battery. When the battery element is assembled, the separator will be at a set thickness (as defined by the cell design) and will exert a given pressure on the active material.

The saturation of the separator is lowered during cell service life because water is lost from the system. Consequently, the compressive force will be reduced and, in the extreme (if the initial compression is low), the separator will lose contact with the active material during the first stage of drying out. This can be avoided by designing the cell to have adequate initial compression and, thereby, good contact will be retained throughout product life.

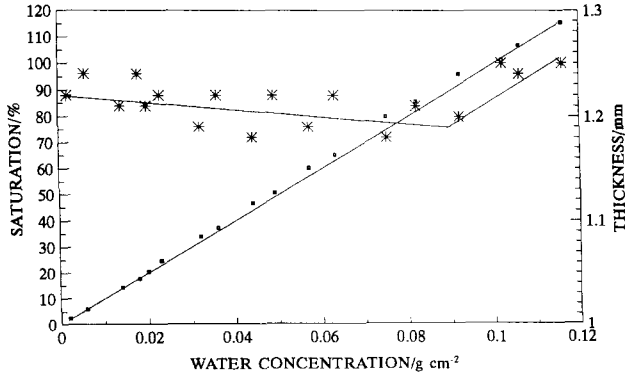

Fig. 11. Saturation vs. thickness, non-glass: (□) saturation, (*) thickness.

Although drainage experiments have been conducted on only one type of GMF separator, such behaviour would be expected to be very dependent on the fibre mix employed. Thus, this type of drainage test should be a valuable aid to characterizing separator materials.

5. Pore size under compression

5.1. Method

One of the standard methods of measuring any separator pore size is the maximum bubble-pressure technique, in which the gas pressure required to force a wetting liquid out of a porous body is measured. This is another measure of the capillary pressure and if the surface tension of the wetting liquid is known, a pore size can be calculated. The method assumes cylindrical pores and measures the size of the largest pore in the sample. (Note, the largest pore has the smallest capillary pressure and will empty first.)

With GMF separators, the material is held under compression in the cell and this would be expected to reduce pore size. Since the effect of compression on pore size has not been reported in the literature, a standard rig used for measuring maximum bubble-pressure was modified by placing the separator test piece between two glass sinters. The pore size of the sinters was much larger than that of the separator under compression. Propan-2-ol was used as the wetting liquid.

5.2. Results

The relationship between maximum pore size and thickness for a range of fibre compositions is given in Fig. 12. As expected, the pore size decreases with decreasing thickness, but in a non-linear manner. The decrease in pore size is approximately 9 μm for a thickness reduction of 1.4–0.3 μm, for all the fibre mixes considered.

5.3. Discussion

The structure of the separator proposed in a previous publication [8] considered the fibres to lie at random, but predominantly in the plane of the sheet (i.e., similar to the structure of a pile of drinking straws) with the largest pore in the z-orientation. These are the pores measured in this test. Compression of the sheet would be expected to have relatively little effect on pore size in the z-direction and this is confirmed in Fig. 12. It can be seen that a reduction in thickness of 50% produces a pore-size reduction of similar magnitude. Further compression results in virtually no change – the pore size remains essentially constant from a thick-

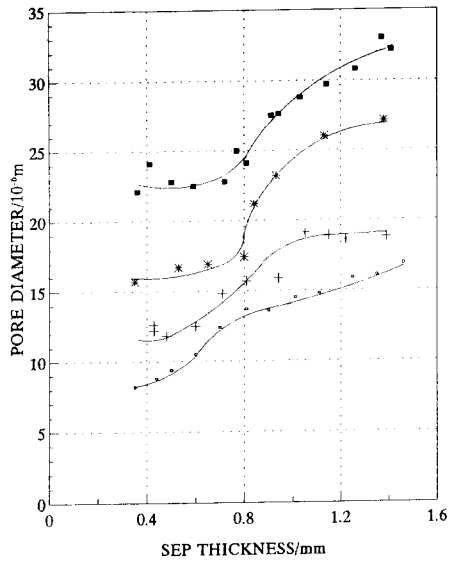

Fig. 12. Maximum pore diameter as a function of compression. Percentage of coarse fibres: (□) 0, (+) 50, (*) 80, (■) 100.

ness of 0.8 mm down to the minimum reached, 0.3 mm.

By comparison, the pore size in the directions of the *x*-, *y*-orientation is greatly affected by pressure, namely, a 15% compression yields a 50% decrease in pore diameter [8]. Again this would be expected from a consideration of the proposed model. The actual values of pore size measured by the maximum bubble-pressure test (in the range 15–35 μm) are very different to those obtained by other methods (such as the sodium penetration test) that are generally used to measure the filtration properties of GMF materials. With the latter methods, a sub-micron pore size is indicated. The reasons for this difference are outside the scope of this paper. Sufficient to say, conventional flooded separators with a measured pore size of 20 μm would be susceptible to 'leading-through' and would give a very short product life.

6. Permeability

6.1. Method

Permeability is a property often measured for various porous media, such as porous rocks and filtration systems [22,23]. It reports the material's resistance to Newtonian fluid flow and, as such, takes into account pore structure and tortuosity. For battery separators, permeability is normally measured along the *z*-orientation, through the plane of the material, by determining the pressure drop of a gas or liquid flow. The value is used to assess the ability of the separator to allow acid transport through the separator, an important function during operation of the cell. In the work reported here, the technique was modified to assess the separator's ability to stop stratification during charging of the cell, i.e., convective flow of acid down the cell during charging of the plates. The technique employed was to seal the separator test piece between two pieces of polycarbonate at the required compression, and then to measure the rate of fluid flow through the separator by use of a calibrated glass tube (Fig. 13). The flow is obviously dependent on the pressure head and this is defined by the height of the liquid in the tube. The method is fully described in the literature and the permeability can be derived from the equation [22,23]:

$$K = \frac{aL\eta}{At\rho g} \ln\left(\frac{h_0}{h_1}\right) \tag{6}$$

By plotting ln h_1 against time, t, a straight line should be obtained with a slope of:

$$\frac{KA\rho g}{aL\eta} \tag{7}$$

where K is the permeability. The units of permeability are m^2, but the values obtained for reasonably porous material are of the order of 10^{-12} m^2 and, conventionally, the non-SI unit, the Darcy, is used, i.e.:

$$1 \text{ Darcy} = 0.987 \times 10^{-12} \text{ m}^2$$

Fig. 14 gives plots of ln h_1 against t for the series of separators examined. All produce good linear plots with values of correlation coefficient $r^2 > 0.998$. These results verify the applicability of the technique for this type of material. A plot of permeability as a function of fibre mix is given in Fig. 15.

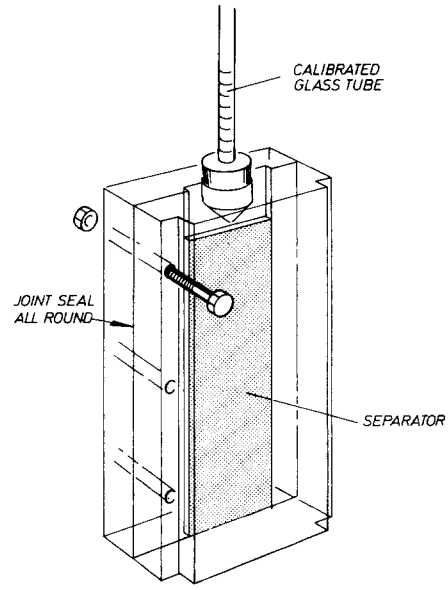

Fig. 13. Test rig for permeability measurement.

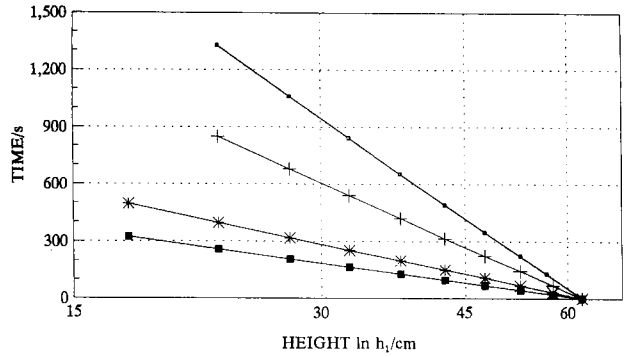

Fig. 14. Verification of the permeability relationship. Percentage of fine fibres: (□) 100, (+) 50, (*) 20, (■) 10.

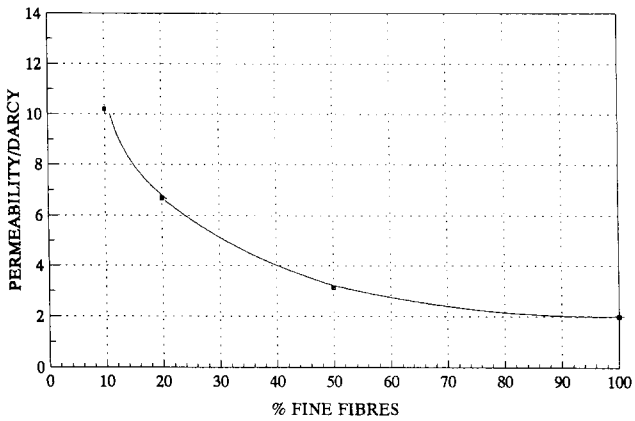

Fig. 15. Permeability as a function of fibre composition.

Table 1
Permeability of some common materials

Material	Darcy
Cigarette	1100
Hair felt	830–1200
Fibre glass	24–51
Sand	20–180
Soil	0.29–14
Leather	0.09–0.12
Slate powder	0.05–0.12
Brick	0.005–0.2
Limestone	0.002–0.4

7. Discussion

As permeability is not a quantity normally encountered, Table 1 lists the values obtained [23] for a range of common materials. The values for GMF are between 2 and 10 Darcy, i.e., somewhat lower than conventional fibre glass at 24–51 Darcy, as might be expected. The trend is non-linear with fibre mix. Thus, there is little advantage in having high contents of fine fibres. No attempt has been made to correlate permeability with a battery-related parameter, but it would be expected to be a measure of the effectiveness of preventing acid stratification. On charge, acid generated in the plate pores sinks to the bottom of the cell before it has a chance to diffuse into the bulk electrolyte and, thereby, causes the development of an acid concentration gradient down the cell. Thus, uneven distribution will reduce the capacity of the cell and, obviously, is to be avoided.

Tuphorn [24] states that GMF-based cells exhibit only 50% of the stratification of flooded cells and, certainly, GMF has a much lower permeability than that of free electrolyte. In a working cell, the situation is complicated because the system becomes three phase (i.e., glass, acid and oxygen) and measuring the permeability in a partially-saturated separator is difficult. It can be postulated, however, that increasing porosity will increase the tortuosity of the liquid phase and, thus, will decrease the permeability.

8. Concluding remarks

One of the major challenges in testing any battery material is to devise simple ex situ tests that bear relevance to performance in the battery. Although the final test must be battery-related, it is often difficult to instrument cells and batteries to obtain basic information on the performance of individual components. It is hoped that the work presented here goes some way towards developing suitable tests for the evaluation of prospective VRLA separators.

Although GMF has now been used as a battery separator for twenty years, the author feels that there is still scope for refinement of its properties so that battery performance can likewise be improved. Already, separators are starting to reach the market with some non-glass component to aid in battery manufacture and give heat-sealing capability. The patent literature contains many examples of VRLA separators that contain particulate silica, and even silica without any GMF. It will be interesting to see how these and similar developments proceed and what inroads they will make into a market which, to date, has been dominated by separators made from 100% glass fibre of micron dimensions.

9. List of symbols

a cross-sectional area of tube (permeability measurement), L^2
A separator cross-sectional area (permeability measurement), L^2
g gravitational constant, LT^{-2}
h wicking height, L
h_0 initial height of liquid column at time zero, L
h_1 height of liquid column at time t, L
h_m maximum wicking height, L

K tortuosity, –
k permeability, L^2
L length of separator, L
P capillary pressure, $ML^{-1}T^{-2}$
r pore radius, L
t time, T
v wicking velocity, LT^{-1}

Greek letters

γ surface tension, MT^{-2}
η viscosity, $ML^{-1}T^{-2}$
θ contact angle, °
ρ density, ML^{-3}
v wicking velocity

Acknowledgements

The author wishes to acknowledge the help of Technical Fibre Products Ltd. who supplied most of the separator materials reported in this paper, and to his colleague, Mr R.P. Bullough, for invaluable help with preparation of the manuscript.

References

[1] B. Culpin, *Chem. Ind. (London), 24* (1989) 826–829.
[2] D.H. McClelland and J.L. Devitt, *US Patent No.* 3 862 861.
[3] K.J. Wandzy and G.W. Taylor, *Battery Man,* (July) (1986) 4–17.
[4] Y. Fujita, *J. Power Sources, 19* (1987) 175.
[5] K. Takahashi, A. Takunaga and M. Tsubota, *Batteries Int.* (Oct.) (1991) 72–73.
[6] G.C. Zguris, D.W. Klauber and N.L. Lifshutz, in T. Keily and B.W. Baxter (eds.), *Power Sources 13,* International Power Sources Symposium Committee, Leatherhead, UK, 1991, pp. 45–57.
[7] *Johns Manville,* Technical Data.
[8] B. Culpin and J.A. Hayman, in L.J. Pearce (ed.), *Power Sources 11,* International Power Sources Symposium Committee, Leatherhead, UK, 1986, pp. 45–66.
[9] H. Tuphorn, *J. Power Sources, 23* (1988) 243.
[10] E.W. Washburn, *Phys. Rev., 17* (1921) 273.
[11] R.H. Muller and D.L. Clegg, *Anal. Chem., 233* (1951) 403.
[12] R.D. Laughlin and J.E. Davis, *Text. Res. J., 31* (1961) 904.
[13] W.B. Palmer, *J. Text. Inst., 44* (1955) T391–400.
[14] R.L. Peek and D.A. McClean, *Ind. Eng. Chem. Anal., 6* (1934) 85.
[15] T.D. Blake, in Th.F. Tadros (ed.), *Surfactants,* Academic Press, London, 1984.
[16] H.G. Bruil and J.J. Van Aartson, *Colloid Polymer Sci., 252* (1974) 32.
[17] D.A. Crouch and J.W. Reitz, *Proc. 3rd Int. Lead/Acid Battery Seminar,* International Lead Zinc Research Organization, Research Triangle Park, NC, USA, 1989, pp. 108–116.
[18] N.R. Morrow, *Bull. Am. Assoc. Pet. Geol., 55* (1971) 514.
[19] N.R. Morrow, *J. Can. Pet. Technol., 10* (1971) 38.
[20] N.R. Morrow, *J. Can. Pet. Technol., 10* (1971) 47.
[21] N.R. Morrow, *J. Can. Pet. Technol., 15* (1976) 49.
[22] F.A.L. Dullien, *Porous Media,* Academic Press, New York, 1979.
[23] A.E. Scheidegger, *The Physics of Flow Through Porous Media,* University of Toronto Press, London, 1960.
[24] H. Tuphorn, *Proc. 3rd Int. Lead/Acid Battery Seminar,* International Lead Zinc Research Organization, Research Triangle Park, NC, USA, 1989, pp. 191–208.